TECHNICAL RESEARCH REPORT

SYSTEMS RESEARCH CENTER

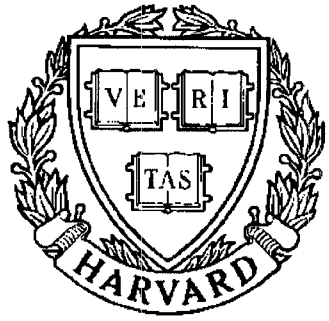

Supported by the National Science Foundation Engineering Research Center Program (NSFD CD 8803012), the University of Maryland, Harvard University, and Industry

Linear Fractional Transformations for the Approximation of Various Uncertainty Sets

by L. Lee and A.L. Tits

TR 91-66

Linear Fractional Transformations for the Approximation of Various Uncertainty Sets

Li Lee and André L. Tits
Electrical Engineering Department and System Research Center
University of Maryland, College Park, MD 20742

ABSTRACT

Recently, it was shown that the structured singular value framework can be extended to the case when information on the phase of the uncertainty is available, and a computable upper bound on the corresponding "phase sensitive structured singular value" was obtained. Here we show that the same bound can be obtained via an entirely different approach, using a family of linear fractional transformations. Extension to various uncertainty "shapes" follows.

1. INTRODUCTION

Robustness analysis is typically based, explicitly or implicitly, on a specific model for the "uncertainty", i.e., for the difference between the nominal model and the true system. Most approaches characterize the uncertainty in terms of a certain norm, without taking advantage of other possibly available information. The structured singular value (SSV) approach [1] models the uncertainty as a collection of "local" uncertain blocks; in the basic SSV setting, uncertainty blocks are either real scalars (parametric uncertainty) or H_∞ transfer functions, and the uncertainty size is characterized by the maximum of the H_∞ norms of the blocks. A "Small μ Theorem" [2] gives a necessary and sufficient condition for stability for all instances of the (structured) uncertainty with norm less than a given bound. Thus, again, aside from the "block structure", the SSV robust stability analysis does not take advantage of any possibly available information on the uncertainty, such as bounds on the phase of the uncertain dynamic blocks.

In [3], it was shown that the SSV framework can readily be extended to account for available phase information on the uncertainty. Specifically, it was shown that a suitably extended small μ theorem holds when the phase of some of the (scalar

complex) blocks is known to lie in a certain (frequency dependent) interval. While, as is the case in general for the classical SSV, the "phase-sensitive" structured singular value does not appear to be easily computable, a computable upper bound to it was also derived in [3].

In [4], computation of the SSV for structures involving real scalar blocks (real or "mixed" μ) was investigated by making use of certain linear fractional transformations (LFTs), leading to a formula for an upper bound. In [5,6] an upper bound to the real or mixed μ, in the form of the optimal value of an optimization problem with suitable convexity properties, was obtained using a different approach, but it was shown that the value of the new bound was in fact identical to that of [4]. The results in [3] are based on an extension of the approach used in [5,6] and the upper bound is given as the value of an optimization problem. The contribution of this paper is twofold. First, the results of [3] are interpreted in terms of suitably defined LFTs; it is observed that other seemingly natural families of LFTs do not appear to lead to upper bounds in the form of a convex optimization problem. Second, the LFT approach suggests direct extensions to other uncertainty "shapes", i.e., complex uncertainty scalar block constrained to lie in various subsets of the complex plane (rather than merely phase constrained).

The balance of this paper is organized as follows. In Section 2, the SSV setup is recalled and the LFT approach to upper bounding the "real μ" is reviewed. In Section 3, instances of uncertainty with phase information are discussed and the concept of phase-sensitive structured singular value, introduced in [3], is recalled. In Section 4, it is shown how the upper bounds obtained in [3] can be related to certain families of LFTs. Extension to other uncertainty shapes is considered in Section 5.

2. PRELIMINARIES

Consider the now standard uncertainty-in-feedback-loop representation of an uncertain system, shown in Fig. 1. Here $P(s)$ and $\Delta(s)$ are H_∞ matrix transfer functions

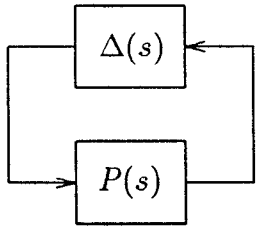

Fig. 1

and $\Delta(s)$ is unknown except that it has a block diagonal structure, with known block dimensions, and selected scalar blocks are known to be real (and independent of s). Complex blocks correspond to dynamic uncertainty, real scalar blocks to parametric uncertainty. Let $\mathcal{X}$ denote the corresponding set of values of $\Delta(\cdot)$.

The Small μ Theorem [2] asserts that the feedback system of Fig. 1 is (well-formed and internally) stable for all Δ of the form specified above, with $\|\Delta\|_\infty \leq 1$, if and only if

$$\sup_\omega \mu_{\mathcal{X}}(P(j\omega)) < 1$$

where, for a complex matrix M, $\mu_{\mathcal{X}}(M)$ is the structured singular value with respect to structure $\mathcal{X}$, given by [1]

$$\mu_{\mathcal{X}}(M) = \begin{cases} 0 & ; \text{if } \det(I - \Delta M) \neq 0 \ \ \forall\, \Delta \in \mathcal{X} \\ \left(\min\limits_{\Delta \in \mathcal{X}} \{\overline{\sigma}(\Delta) : \det(I - \Delta M) = 0\}\right)^{-1} & ; \text{otherwise.} \end{cases}$$

Computation of $\mu_{\mathcal{X}}$ is a challenging issue. It is easily shown that

$$\mu_{\mathcal{X}}(M) \leq \inf_{D \in \mathcal{D}} \overline{\sigma}(DMD^{-1}) \tag{1}$$

where $\overline{\sigma}$ denotes the largest singular value and $\mathcal{D}$ the set of nonsingular matrices that commute with $\mathcal{X}$. The optimization problem in (1) has convexity properties that makes it computationally tractable and extensive numerical experimentation suggests that; if none of the (scalar) blocks of matrices in $\mathcal{X}$ is constrained to be real, inequality (1) is always close to being an equality. This is no longer the case when real scalars (i.e., parametric uncertainty) are present, however, and this motivated the LFT approach proposed by Doyle in [4].

To keep matters simple, consider the block diagram of Fig. 1 with $\Delta(s)$ taking values in

$$\tilde{\mathcal{X}} = \{\text{block diag}(\delta, \Delta_2) : \ \delta \in \mathbb{R}, \ \Delta_2 \in \mathbb{C}^{2\times 2}\}.$$

Also consider the block diagram of Fig. 2 where $P(S)$ is as above and, for all s,

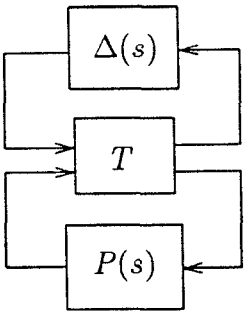

Fig. 2

$\Delta(s) \in \mathcal{X}$, given by

$$\mathcal{X} = \{\text{block diag}(\delta, \Delta_2) : \ \delta \in \mathbb{C}, \ \Delta_2 \in \mathbb{C}^{2\times 2}\}$$

(note the difference with $\tilde{\mathcal{X}}$), and T is a constant "connection" matrix given by

$$T = T(c) = \begin{pmatrix} jC & I \\ (I - C^2)^{\frac{1}{2}} & O \end{pmatrix}$$

with

$$C = \text{diag}(c, 0, 0)$$

and $c \in (-1, 1)$. Clearly, this system is (well-formed and internally) stable if either the upper loop or the lower loop is open, and stability of the overall system (with

both loop closed) is equivalent to that of the systems of Fig. 3 and of Fig. 4 where F_ℓ and F_u (for lower and upper) are defined by the linear fractional transformations

$$\begin{aligned} F_\ell(T, P(s)) &= jC + P(s)(I - C^2)^{\frac{1}{2}} \\ F_u(T, \Delta(s)) &= (I - C^2)^{\frac{1}{2}}\Delta(s)(I - jC\Delta(s))^{-1} \end{aligned}$$

Thus, in view of the Small μ Theorem, the system with both loops closed is stable

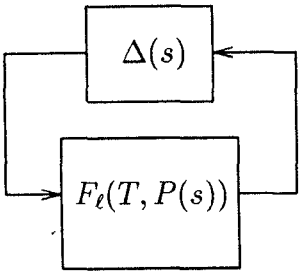

Fig. 3

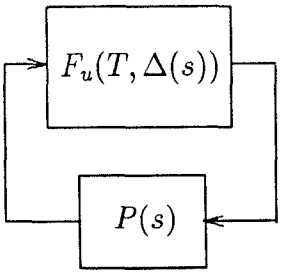

Fig. 4

for all $\Delta(\cdot)$ with $\|\Delta\|_\infty \leq 1$, $\Delta(s) \in \mathcal{X}$ for all s, if and only if

$$\sup_\omega \mu_{\mathcal{X}}(F_\ell(T(c), P(j\omega))) < 1.$$

On the other hand LFTs map disks to disks and when $\Delta(j\omega)$ ranges over $\mathcal{X}$, with $\|\Delta\|_\infty \leq 1$, $F_u(T, \Delta(j\omega))$ ranges over $\mathcal{X}$ with the bottom right block unaffected but the scalar top left block now ranging over a disk such as those shown in Fig. 5 (these disks are parametrized in values of $c \in (-1, 1)$). Since each one of these disks covers

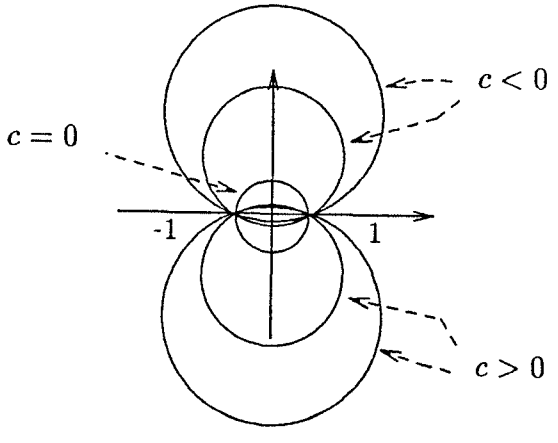

Fig. 5

the $[-1, 1]$ interval of the real line, stability of the overall system for $\Delta(j\omega)$ ranging over $\mathcal{X}$, $\overline{\sigma}(\Delta(j\omega)) \leq 1$ implies stability of the system of Fig. 1 with $\Delta(j\omega)$ ranging over $\tilde{\mathcal{X}}$, with $\overline{\sigma}(\Delta(j\omega)) \leq 1$, i.e., in view of the Small μ Theorem, $\forall\, c \in (-1, 1)$,

$$\sup_\omega \mu_{\mathcal{X}}(F_\ell(T(c), P(j\omega))) < 1 \Longrightarrow \sup_\omega \mu_{\tilde{\mathcal{X}}}(P(j\omega))) < 1. \tag{2}$$

Suppose now that the nominal plant $P(s)$ is memoryless, say, $P(s) = M$, a constant matrix. Then (2) becomes

$$\mu_{\mathcal{X}}(F_\ell(T(c), M)) < 1 \Longrightarrow \mu_{\tilde{\mathcal{X}}}(M) < 1.$$

Since $\mu(\cdot)$ is positively homogeneous, it follows that, for any $\gamma > 0$, $c \in (-1, 1)$

$$\mu_{\mathcal{X}}(F_\ell(T(c), \frac{M}{\gamma})) < 1 \Longrightarrow \mu_{\tilde{\mathcal{X}}}(M) < \gamma,$$

i.e.,

$$\mu_{\tilde{\mathcal{X}}}(M) \leq \inf_{\gamma>0}\{\inf_{c\in(-1,1)} \mu_{\mathcal{X}}(F_\ell(T(c), \frac{M}{\gamma})) < 1\}.$$

Since, as is easily verified, for all $D \in \mathcal{D}$,

$$DF_\ell(T(c), \frac{M}{\gamma})D^{-1} = F_\ell(T(c), D\frac{M}{\gamma}D^{-1}),$$

this yields, in view of (1)

$$\mu_{\tilde{\mathcal{X}}}(M) \leq \inf_{\gamma>0}\{\inf_{\substack{c\in(-1,1)\\ D\in\mathcal{D}}} \overline{\sigma}(F_\ell(T(c), D\frac{M}{\gamma}D^{-1})) < 1\}, \tag{3}$$

which was obtained in [4]. In [6], it was shown that the right hand side of (3) is equal to

$$\sqrt{\inf_{D\in\mathcal{D}} \inf_{G\in\mathcal{G}} \overline{\lambda}(M_D^H M_D + j(M_D^H G - G^H M_D))} \tag{4}$$

with $M_D = DMD^{-1}$ and $\mathcal{G} = \{\text{diag}(g, 0, 0) : g \in \mathbb{R}\}$. This bound is first derived in [6] by an entirely different approach. The advantage of (4) is that it can be transformed into a convex optimization problem (see [6]).

In Section 4 below, the LFT approach reviewed here will be extended to handle uncertainty with phase information, and bounds obtained in [3] will be recovered.

3. UNCERTAINTY WITH PHASE INFORMATION

Various shapes of scalar complex uncertainty with phase bounds are shown in Figs. 6 through 11 (some of them were considered in [3]). Phase bounds may come from partial knowledge of the uncertainty, from experimental data, or from the result of an estimation procedure [7]. These shapes may also be adequately used to describe certain parametrically modeled uncertainty with correlated uncertain parameters. An example is given in Figs. 12 and 13 where values of the transfer function

$$\frac{a(s+b)}{s^2 + 2cs + 1} \tag{5}$$

with parameters a, b, c lying in certain intervals are shown at two frequencies.

For each uncertainty case we can define the corresponding $\mathcal{X}$, denoted as $\mathcal{X}^\theta$. Thus the "phase sensitive singular value" is defined (see [3]) by the same formula as $\mu_{\mathcal{X}}(M)$ with $\mathcal{X}$ being replaced by $\mathcal{X}^\theta$. By an extension of the Small μ Theorem the inequality

$$\sup_\omega \mu_{\mathcal{X}^\theta}(P(j\omega)) < 1$$

is a necessary and sufficient condition on stability for all $\Delta \in \mathcal{X}^\theta$, with $\|\Delta\|_\infty \leq 1$.

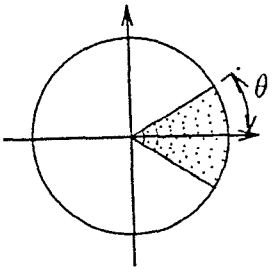

Fig. 6: right sector uncertainty

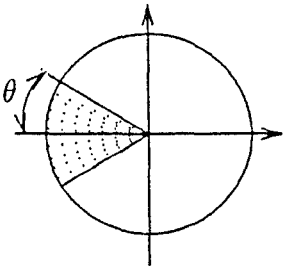

Fig. 7: left sector uncertainty

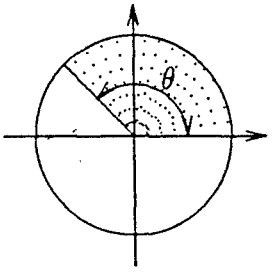

Fig. 8: upper sector uncertainty

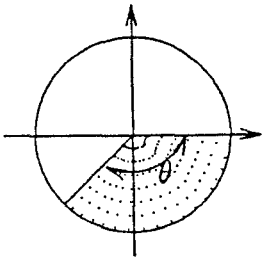

Fig. 9: lower sector uncertainty

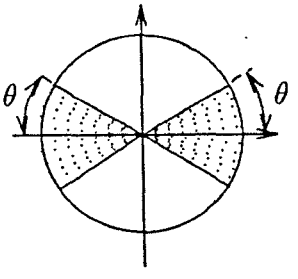

Fig. 10: butterfly shaped uncertainty

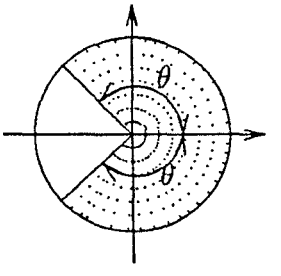

Fig. 11

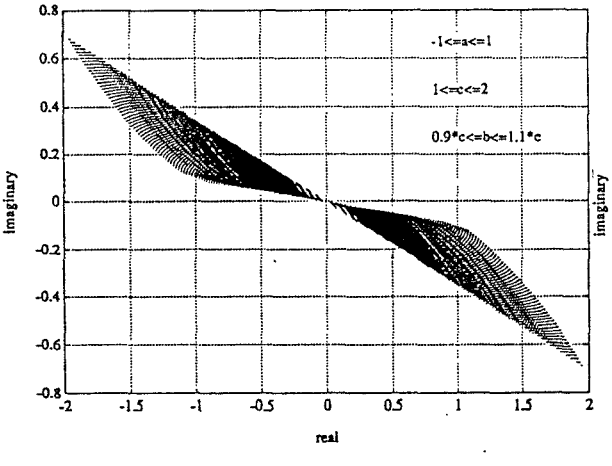

Fig. 12 Uncertainty set for (5) at $\omega = 0.1$

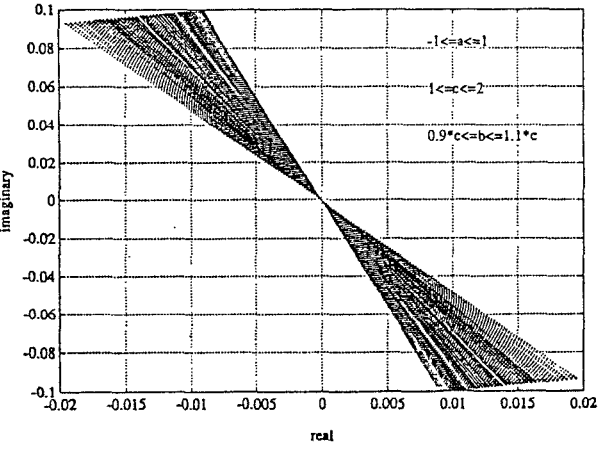

Fig. 13 Uncertainty set for (5) at $\omega = 10$

4. UPPER BOUNDS ON μ FOR VARIOUS UNCERTAINTY SHAPES

In this section, we show how an LFT based approach analogous to that used by Doyle in [4] in the real μ case (and reviewed in Section 2 above) can be used to obtain an upper bound on μ^θ.

Consider again Fig. 2 with constant matrix T now given by

$$T = T(\alpha, \beta) = \begin{pmatrix} F(I + F^H F)^{-\frac{1}{2}} & I \\ (I + F^H F)^{-\frac{1}{2}} & O \end{pmatrix}$$

with

$$F = F(\alpha, \beta) = \mathrm{diag}(\alpha(1 + j\beta), 0, 0) \qquad \alpha,\ \beta \in \mathbb{R}.$$

For such T, and complex matrices M and Δ, we now have

$$\begin{aligned} F_\ell(T, M) &= (M + F)(I + F^H F)^{-\frac{1}{2}} \\ F_u(T, \Delta) &= (I + F^H F)^{-\frac{1}{2}} \Delta [I - F(I + F^H F)^{-\frac{1}{2}} \Delta]^{-1} \end{aligned}$$

The argument used in Section 2 is still valid here, except that the (1,1) entry of $F_u(T, \Delta)$ is now given by

$$\frac{\delta}{\sqrt{1 + \alpha^2(1 + \beta^2)} - \alpha(1 + j\beta)\delta},$$

and when δ ranges over the unit disk centered at the origin, this quantity ranges over a disk centered at $\alpha(1 - j\beta)$ with radius $\sqrt{1 + \alpha^2(1 + \beta^2)}$, as shown in Fig. 14 for $\alpha = 1$ and in Fig. 15 for α ranging over $[0, 1]$. It can be seen that for any $\alpha \geq 0$ and $|\beta| \leq \cot\theta$, this disk covers the right sector uncertainty of Fig. 6. It follows that (see argument used in Section 2), for any constant matrix M

$$\mu^\theta_{\text{right}}(M) := \mu^\theta(M) \leq \inf_{\gamma > 0} \{\gamma : \inf_{D \in \mathcal{D}} \inf_{\substack{\alpha \geq 0 \\ |\beta| \leq \cot\theta}} \overline{\sigma}(F_\ell(T(\alpha, \beta), \frac{M_D}{\gamma})) < 1\}. \tag{6}$$

This upper bound can be transformed into an optimization problem similar to (4), which again has suitable convexity properties.

Theorem 1.

$$\mu^\theta_{\text{right}}(M) \leq \sqrt{\max\{0,\ \inf_{D \in \mathcal{D}} \inf_{\substack{\alpha \geq 0 \\ |\beta| \leq \cot\theta}} \overline{\lambda}(M_D^H M_D + M_D^H F(\alpha, \beta) + F(\alpha, \beta)^H M_D)\}} \tag{7}$$

and the right hand side is equal to the right hand side in (6).

Proof. Basically the proof follows the same algebraic manipulation as in [6]. Eqn.(7) comes from the following sequence of equivalent inequalities:

For $\forall D \in \mathcal{D}$, $\forall \alpha \geq 0$, $|\beta| \leq \cot\theta$, and since $\gamma > 0$,

$$\begin{aligned}
& \overline{\sigma}[F_\ell(T(\alpha,\beta), \tfrac{M_D}{\gamma})] < 1 \\
\iff\ & \overline{\sigma}[(\tfrac{M_D}{\gamma} + F)(I + F^H F)^{-\frac{1}{2}}] < 1 \\
\iff\ & [(\tfrac{M_D}{\gamma} + F)(I + F^H F)^{-\frac{1}{2}}]^H [(\tfrac{M_D}{\gamma} + F)(I + F^H F)^{-\frac{1}{2}}] < I \\
\iff\ & (\tfrac{M_D^H}{\gamma} + F^H)(\tfrac{M_D}{\gamma} + F) < I + F^H F \\
\iff\ & [M_D^H M_D + M_D^H(\gamma F) + (\gamma F)^H M_D] < \gamma^2 I \\
\iff\ & \overline{\lambda}(M_D^H M_D + M_D^H F + F^H M_D) < \gamma^2.
\end{aligned}$$

Q.E.D.

For the left sector uncertainty of Fig. 7, α must range over the negative real line, yielding

$$\mu^\theta_{\text{left}}(M) \leq \sqrt{\max\{0,\ \inf_{D\in\mathcal{D}} \inf_{\substack{\alpha\leq 0 \\ |\beta|\leq\cot\theta}} \overline{\lambda}(M_D^H M_D + M_D^H F(\alpha,\beta) + F(\alpha,\beta)^H M_D)\}} \qquad (8)$$

The butterfly-shaped uncertainty in Fig. 10 is the union of those in Figs. 6 and 7, therefore,

$$\mu^\theta_{\text{butterfly}}(M) = \max\{\mu^\theta_{\text{right}}(M),\ \mu^\theta_{\text{left}}(M)\}$$

and is bounded by the maximum of two upper bounds in (7) and (8). For upper and lower sector uncertainty as in Fig. 8 and 9, a similar family of LFTs can be used, yielding upper bounds on $\mu^\theta_{\text{upper}}(M)$ and $\mu^\theta_{\text{lower}}(M)$ of the same form as in (7), except $\beta \geq -\cot\theta$ for the upper case and $\beta \leq \cot\theta$ for the lower case. Consequently, an upper bound for the uncertainty set of Fig. 11 is given by the "max" between these two upper bounds.

An alternative LFT which deals with the butterfly-shaped uncertainty as a whole would be the following natural extension of the real uncertainty case. Define

$$T = T^\theta(c) = \begin{pmatrix} jC & I \\ \Phi(C,\theta) & O \end{pmatrix}$$

where

$$\Phi(C,\theta) = |C| \cdot \text{diag}(\sin\theta, 0, 0) + (I - C^2 \cdot \text{diag}(\cos^2\theta, 0, 0))^{\frac{1}{2}}$$

with $|C| = \text{diag}(|c|, 0, 0)$. Then

$$\mu_{\mathcal{X}}(M) \leq \inf_{\gamma>0}\{\gamma : \inf_{\substack{c\in(-1,1) \\ D\in\mathcal{D}}} \overline{\sigma}(F_\ell(T^\theta(c), \frac{M_D}{\gamma})) < 1\}.$$

Note that when $\theta = 0$, $\Phi(C,0) = (I - C^2)^{\frac{1}{2}}$, it becomes the real uncertainty case. However, because now $F_\ell(T, M) = jC + M\Phi(C,\theta)$, following the approach used in the proof, we have

$$\overline{\sigma}[F_\ell(T^\theta(c), \tfrac{M_D}{\gamma})] < 1 \qquad \iff$$
$$\tfrac{M_D^H M_D}{\gamma^2} + \tfrac{M_D^H}{\gamma} jC\Phi(C,\theta)^{-1} + (jC\Phi(C,\theta)^{-1})^H \tfrac{M_D}{\gamma} + [I + (\Phi(C,\theta)^{-1})^H (C^2 - I)\Phi(C,\theta)^{-1}] < I.$$

Since the term in brackets is positive-semidefinite, the above implies

$$M_D^H M_D + M_D^H(\gamma j C\Phi(C,\theta)^{-1}) + (\gamma j C\Phi(C,\theta)^{-1})^H M_D < \gamma^2 I$$

but not conversely. Since for any $\theta \in [0, \frac{\pi}{2}]$, the mapping

$$\frac{c}{|c|\sin\theta + \sqrt{1-c^2\cos\theta^2}} : (-1,1) \longrightarrow \mathbb{R}$$

is bijective and since $\gamma > 0$, it follows that

$$\sqrt{\max\{0, \inf_{G\in\mathcal{G}} \overline{\lambda}[M_D^H M_D + j(M_D^H G - G^H M_D)]\}} \leq \inf_{\gamma>0}\{\gamma : \inf_{\substack{c\in(-1,1)\\ D\in\mathcal{D}}} \overline{\sigma}(F_\ell(T^\theta(c), \frac{M_D}{\gamma})) < 1\}, \tag{9}$$

with $\mathcal{G}$ as in (4), to be compared to the *equality* asserted in Theorem 1. Inequality (9) does not yield an upper bound on $\mu^\theta_{\text{butterfly}}(M)$.

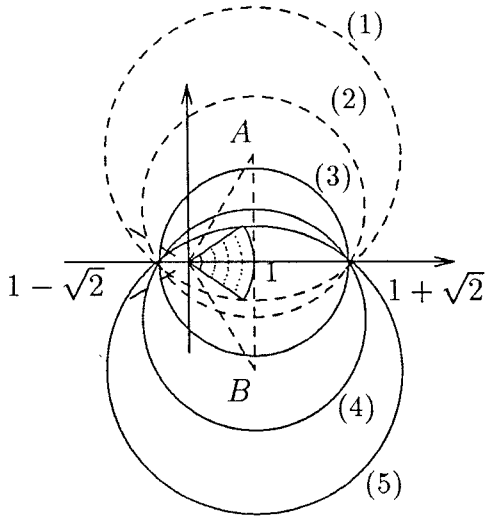

(1): $\beta = -\cot\theta$
(2): $-\cot\theta < \beta < 0$
(3): $\beta = 0$
(4): $0 < \beta < \cot\theta$
(5): $\beta = \cot\theta$
$A : \alpha(1 + j\cot\theta)$
$B : \alpha(1 - j\cot\theta)$

Fig. 14 $(\alpha = 1)$

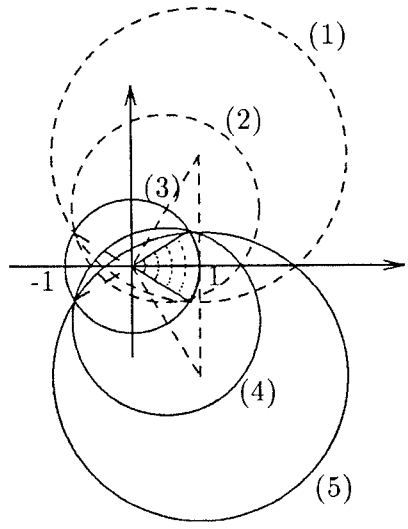

(1),(2): $\beta = -\cot\theta$
(4),(5): $\beta = \cot\theta$
(1),(5): $\alpha = 1$
(2),(4): $0 < \alpha < 1$
(3): $\alpha = 0$

Fig. 15

5. EXTENSION

Upper bounds on μ obtained above can be easily extended to scalar uncertainties constrained in more general shapes than those considered in the paper. This can be done by properly adjusting the ranges for α and β. For example, in (7) when α is assumed to take value in $[0, 1]$ instead in $[0, \infty)$, then the solution to the corresponding optimization problem gives an upper bound on μ associated with uncertainty shape being the intersection of all disks in Fig. 15. Further extension to handle block uncertainty is possible based on the ideas introduced in [8].

REFERENCES

[1] J.C. Doyle, "Analysis of Feedback Systems with Structured Uncertainties," *Proc. IEE-D* 129 (1982), 242–250.

[2] J.C. Doyle, J.E. Wall & G. Stein, "Performance and Robustness Analysis for Structured Uncertainty," in *Proc. 21st IEEE Conf. on Decision and Control*, Orlando, Florida, December 1982, 629–636.

[3] L. Lee, A.L. Tits & M.K.H. Fan, "Robustness under Uncertainty with Phase Information," in *Proc. of the 28th Conf. on Decision and Control*, Tampa, Florida, December 1989, 2315–2316.

[4] J.C. Doyle, "Structured Uncertainty in Control System Design," in *Proceedings of the 24th IEEE Conference on Decision and Control*, Fort Lauderdale, Florida, December 1985, 260–265.

[5] M.K.H. Fan, A.L. Tits & J.C. Doyle, "Robustness in the Presence of Joint Parametric Uncertainty and Unmodeled Dynamics," in *Proc. of the 1988 American Control Conference*, Atlanta, Georgia, June 1988, 1195–1200.

[6] M.K.H. Fan, A.L. Tits & J.C. Doyle, "Robustness in the Presence of Mixed Parametric Uncertainty and Unmodeled Dynamics," *IEEE Trans. Automat. Control* 36 (1991), 25–38.

[7] A.P. Loh, G.O. Correâ & I. Postlethwaite, "Estimation of Uncertainty bounds for Robustness Analysis ," *IEE Proceedings Pt. D* 134 (Jan., 1987), 9–16.

[8] L. Lee & A.L. Tits, "On Phase Information in Multivariable Systems," in *Proceedings of MTNS 91*, H. Kimura & S. Kodama, eds., 1992, to appear.